Journal Name

Dynamic Article Links ▶

ARTICLE TYPE

Designing metal hydride complexes for water splitting reactions: A molecular electrostatic potential approach

K. S. Sandhya,[a] and Cherumuttathu H. Suresh*[a]

Abstract:

The hydridic character of octahedral metal hydride complexes of group VI, VII and VIII has been systematically studied using molecular electrostatic potential (MESP) topography. The absolute minimum of MESP at the hydride ligand (V_{min}) and MESP value at the hydride nucleus (V_H) are found to be very 10 good measures of the hydridic character of the hydride ligand. The increasing/decreasing electron donating feature of the ligand environment is clearly reflected on the increasing/decreasing negative character of V_{min} and V_H. The formation of an outer sphere metal hydride-water complex showing H...H dihydrogen interaction is supported by the location and value of V_{min} near the hydride ligand. A higher negative MESP suggested lower activation energy for H_2 elimination. Thus, MESP features provided a 15 way to fine tune the ligand environment of a metal-hydride complex to achieve high hydridicity for the hydride ligand. The applicability of MESP based hydridic descriptor in designing water splitting reactions is tested for group VI metal hydride model complexes of tungsten.

Introduction

Transition metal hydride complexes play an important catalytic 20 role in a variety of synthetically important reactions as well as in biological reactions.[1-6] Several transition metal hydride complexes catalyse dihydrogen formation in the presence of reducing agents.[7-13] Recently, Milstein *et. al.* reported the discovery of a monomeric aromatic pincer Ru(II) hydride catalyst 25 for water splitting reaction.[14] This catalyst activates the O-H bond for water splitting through aromatization-dearomatization steps involving a PNN pincer ligand and the metal center.[15, 16] Mechanistic studies from our group have shown that the hydride ligand of the Milstein catalyst facilitates H...H dihydrogen 30 interaction with water molecule leading to an outer sphere mechanism for H_2 elimination.[17] Similarly, hydride donor ability has been invoked to explain the reaction of $W(H)(NO)(CO)(PMe_3)_3$ with various alcohols, under mild condition to liberate dihydrogen.[18] Very recently we have 35 shown that H...H dihydrogen bonded complexes are reactant species in the associative and migratory insertion mechanisms of $MH(NO)(CO)_2(PH_3)_2$, $MH(NO)(CO)(PH_3)_3$ and $MH(NO)(CO)(PH_3)_4$ (M = Cr, Mo and W) complexes for H_2 elimination.[19] Peruzzini *et al* studied the dihydrogen interaction 40 between the metal hydride complexes [(^{tBu}PCP)Ni(H)] and

Inorganic and Theoretical Chemistry Section, CSTD, CSIR-National Institute for Interdisciplinary Science and Technology, Trivandrum-695019, India
Phone: +91-471-2535506; Fax: +91-471-2491712
45 *E-mail:sureshch@gmail.com*

$[CpW(H)(CO)_3](^{tBu}PCP=2,6- C_6H_3(CH_2P^{tBu}_2)_2)$ and reported the evolution of H_2 upon the increase in reaction temperature.[20] The 50 H_2 elimination is also reported for four-, five- and seven-coordinated transition metal hydride complexes.[21-23] In the case of four-coordinated complex of CpRu(dppe)H (dppe = $Ph_2PCH_2CH_2PPh_2$) with HA (A = acceptor), an equilibrium between dihydrogen bonded complex and cationic dihydrogen 55 complex has been monitored at low temperature by NMR spectroscopy.[24] It is noteworthy that such systems are precursor for (η^2-H_2) Kuba's dihydrogen complexes.[25] Moreover, these dihydrogen complexes are potential candidates for hydrogen storage applications, crystal engineering, catalyst designing and 60 many other applications.[26, 27]

The present study mainly focuses on the analysis of molecular electrostatic potential (MESP) and its topography in metal hydride complexes. MESP features have been successfully employed to understand many important fundamental problems 65 in chemistry.[28-31] For example, MESP is used for the study of the site for electrophilic or nucleophilic attack, intermolecular reactivity, non covalent interaction, electronegativity of elements, substituent effects and various chemical phenomena.[32-37] Gadre *et al.* derived MESP topographical features for probing the 70 intermolecular distance in hydrogen bonded complexes of the type D-H...A (D = N, O, B, C, F, S, Cl; A = F).[38] Galabov *et al.* used MESP at hydride nucleus for characterizing the reactivity of substituted aromatic molecules.[39-41] Previously proton affinity, thermodynamic and various spectroscopic methods have been 75 used to characterize electron donating character of a hydride ligand of metal hydride complexes.[42-45] In the present study a

MESP based approach will be presented to characterize the hydridic character of a hydride ligand in a metal complex and the formation of electron rich hydride ligands in some metal hydride complexes will be revealed for the facile liberation of dihydrogen from water.

Theoretical methods

The MESP, $V(\mathbf{r})$ at a point $\mathbf{r}$ in atomic units is given by eq. 1 where $\rho(\mathbf{r})$ is the electronic charge density and N is the total number of nuclei in the molecule.[29] $V(\mathbf{r})$ is a real physical quantity

$$V(\mathbf{r}) = \sum_{A}^{N} \frac{Z_A}{|\mathbf{r} - \mathbf{R}_A|} - \int \frac{\rho(\mathbf{r}')d^3r'}{|\mathbf{r} - \mathbf{r}'|} \quad (1)$$

and can either be positive or negative depending upon whether the effect of nuclei (first term in eq. 1) or electron (second term in eq. 1) dominates over the other. The MESP at the nucleus A of a molecule (V_A) can be obtained by dropping out the nuclear contribution due to Z_A from eq. 1.[29] In MESP topography analysis, negative-valued minima appear at the electron rich regions of molecules. In this work, a MESP minimum located near a hydride ligand of the metal hydride complexes is denoted as V_{min} and the notation V_H is used to represent the MESP value at the hydride nucleus.
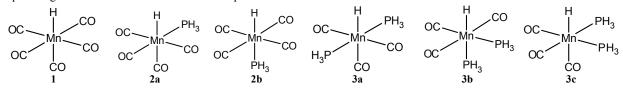
Gaussian09 suite of quantum chemical programs is used for performing all the calculations.[46] Geometry optimization of all the complexes are performed using the hybrid density functional B3LYP.[47, 48] The LanL2DZ basis set is chosen for transition metals which also incorporates the effective core potential (ECP) of Hay and Wadt with additional f polarization functions.[49, 50] For all other atoms, 6-31G(d, p) basis set is selected.[51, 52] Further, a triple zeta split-valence basis set 6-311++G(d,p) was used for atoms other than transition metals in single point calculation to obtain more accurate description of the activation barrier for H_2 elimination step. All the optimized structures were confirmed as either minima or transition state by vibrational frequency calculation. All the reported transition states show one imaginary frequency and all other structures have no imaginary frequency. IRC calculations are conducted for confirming the connectivity of the transition states to the respective minimum energy structures.[53] In the case of water adducts, counter poise method was used to evaluate the BSSE correction for the interaction energy.[54] Effect of phosphine coordination is mainly modelled using PH_3 ligand while several test cases have been modelled using ligands such as trimethyl-, triethyl-, and triphenyl phosphines.

Results and Discussion

The octahedral metal hydride complexes of Mo and W from group VI, Mn and Re from group VII and Fe and Ru from group VIII given in Fig. 1 are selected for this study. At least one phosphine ligand is selected for most of the complexes because they have high synthetic applicability in tuning steric and electronic properties of the complexes.[55-58] In the case of Mn complexes, various possible combinations of CO and PH_3 ligands are considered along with chelate 1, 2-bis(phosphino)ethane ligands and N_2 ligand. Remaining complexes, consists of various types of ligands, *viz.* CN, Cl, F, NO, CH, N_2, NCO, CO, SiH_3, P- and N-based bidentate, cyclic NC_3H_4 and $N_2C_2H_4$ ligands. The **1** and **11** contain no phosphine ligand. Most of the synthetically known complexes consist of triphenyl/trimethyl/isopropyl phosphine ligands while our calculation replaces them with unsubstituted phosphine which reduces the computational cost. For a limited number of tungsten complexes, higher derivatives have been computed using bulky triethyl-, trimethyl- and triphenyl phosphine ligands. Compounds similar to **1**, **2a**, **3a**, **3b** and **4a** have been reported in the literature[18]. The **7**, **8** and **9** are made up of bidentate chelating phosphine ligand.

Among the complexes reported in Fig. 1, for the higher derivatives (with bulky phosphine ligands), the literature shows the following aspects on their properties/reactivity. Through NMR measurements, they calculated that the effective charge of hydride in $MnH(CO)_4PPh_3$ (the higher derivative of **2a**) is -0.40 e, which was higher than **1**. Darensbourg *et. al.* reported the expoxide ring opening by H ligand in the chelated Mn complex $MnH(dppp)(CO)_3$ where dppp is 1,3,-bis(diphenylphosphino)- propane))[42]. Nietlispach *et al.* synthesized a series of Re-hydride complexes $ReH(CO)_n(PR_3)_{5-n}$ (n=5, 4, 3, 2, 1 and R = Ph, CH_3) and showed that hydridic character depends on the increasing number of phosphine ligand and they undergo insertion reactions with CO, CO_2, CS_2, and ketones.[43] Berke *et. al* studied the unusual insertion behaviour in the metal-H bond of chelated $MoH(dmpe)_2NO$ complex (dmpe = 1,2-bis(dimethyl phosphino-)) with inactive imines[44] and argued that the high propensity of the dmpe ligand towards imine was due to the chelating effect of cis- bidentate phosphine ligand which enhanced the hydridic character compared to $MoH(NO)(CO)_2(PR_3)_2$ and $MoH(NO)(CO)(PR_3)_3$. Abramov *et. al.* noted that by substituting PPh_3 in place of CO group in system **1** gives higher hydridic character to the hydride ligand.[59] The $MoH(CO)_n(PR_3)_{5-n}$ (n = 3, 2, 0) and $WH(CO)_n(PR_3)_{5-n}$ (n = 3, 2, 1) complexes have shown hydride transfer activity to CO, CO_2, CS_2, acetylene and ketones[44, 60, 61] Hillhouse and Haymore synthesised $WH(NO)(CO)_2(PR_3)_2$ (R = C_6H_5 and $CH_3C_6H_4$) and showed that these complexes undergo various type of insertion and elimination reactions with small molecules.[62] Recently we have described the insertion behaviour of water with bis- and, tris- phosphine Cr, Mo and W hydride complexes for H_2 elimination.[19] The enhancement in the hydridic character of a metal hydride complex is strongly related to the weakening of the metal-H bond and suggests that a metal-H bond is susceptible for various reactions such as insertion, elimination, proton donation and proton transfer.
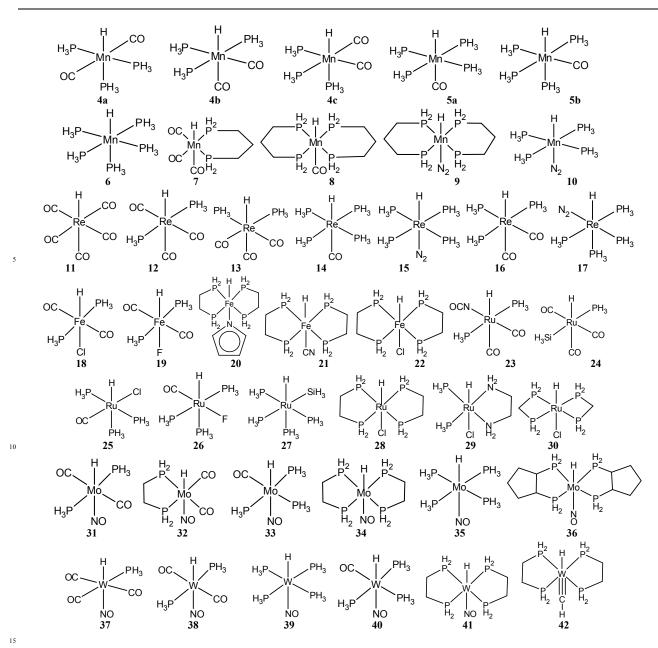
Fig. 1 Schematic representations of group VI, VII and VIII octahedral metal hydride complexes.

Structural features of Mo, W, Mn, Re, Fe and Ru hydride complexes

All the complexes acquired pseudo octahedral geometry (some representative structures are listed in Fig. 2), in which most of them possess slight inclination of equatorial ligands to the hydride ligand (the average ligand-metal-H angle, δ is 85º). The metal-H (M-H) distance is found to be in the range 1.506 to 1.897 Å which can be correlated to the position of the metal in the periodic table and the associated ligands in the complex (Table 1). A general trend of increase in M-H distance with increase in the size of the metal is observed in each group. The M-H distance increases to the maximum for Mo and W complexes and suggests easy M-H bond dissociation for group VI complexes. Minor discrepancies in the general trend of M-H distance can be observed in cases of (Mo, W) complexes such as (**31**, **37**), (**33**, **38**) and (**35**, **40**). This can be attributed to variations in the ligand
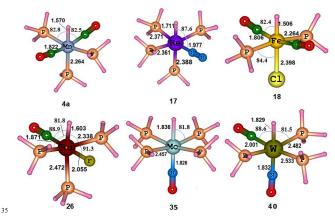

Fig. 2 Structures of a representative set of metal-hydride complexes. Bond distance in Å and bond angles in degree.

Table 1. Metal hydrogen distance in Å for all the complexes.

Models	d_{M-H}	models	d_{M-H}	models	d_{M-H}	models	d_{M-H}	models	d_{M-H}	models	d_{M-H}
1	1.574	**5a**	1.619	**13**	1.745	**22**	1.533	**31**	1.814	**40**	1.829
2a	1.581	**5b**	1.584	**14**	1.764	**23**	1.632	**32**	1.814	**41**	1.843
2b	1.545	**6**	1.604	**15**	1.725	**24**	1.654	**33**	1.823	**42**	1.897
3a	1.592	**7**	1.575	**16**	1.755	**25**	1.605	**34**	1.838		
3b	1.556	**8**	1.619	**17**	1.711	**26**	1.603	**35**	1.836		
3c	1.586	**9**	1.608	**18**	1.506	**27**	1.632	**36**	1.839		
4a	1.570	**10**	1.606	**19**	1.530	**28**	1.609	**37**	1.812		
4b	1.601	**11**	1.731	**20**	1.557	**29**	1.613	**38**	1.822		
4c	1.567	**12**	1.747	**21**	1.555	**30**	1.602	**39**	1.840		

environment. If the ligand environment is same as in the case of **33** and **40**, the size of the metal is decisive for the M-H distance. Another observation is that in complexes having CO in trans orientation to PH₃, the M-P distance show significant elongation which can be attributed to the mutual trans influence between the ligands (eg. **40** in Fig. 2).[63]

MESP features of the representative system

In general, negative MESP regions are located in electron rich regions of a molecule.[29] Since the hydride ligand is negatively charged, the M-H region of a metal hydride complex is expected to be electron rich. In order to illustrate this, MESP features of the representative system **31** are presented in Fig. 3. Fig. 3a shows a MESP plane passing through M-H and M-NO bonds. The violet regions clearly indicate concentration of electrons around the hydride ligand as well as around the oxygen of the NO ligand. The MESP isosurface depicted in Fig. 3b is useful to obtain a 3D view of the electron concentration around the hydride ligand. The most negative-valued MESP point (V_{min}) is also noted in Fig. 3b for the hydride and NO ligands. The negative MESP region around NO can be correlated to the lone pair region of its oxygen.[64]
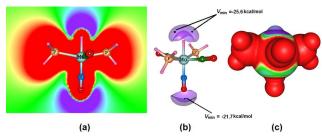

Fig. 3 Electrostatic potential features of **31**. (a) MESP plotted on a plane. (b) MESP isosurface plot, value -22.0 kcal/mol (c) MESP on van der Waals (value range from -0.02 au (violet) to 0.02 au (red)).

It is noteworthy that V_{min} of the hydride ligand (-25.6 kcal/mol) is more negative than V_{min} of NO ligand (-21.7 kcal/mol). This suggests a highly localized electron distribution around the hydride ligand where the electron concentration is higher than the NO oxygen. The MESP feature showing two V_{min} points for the hydride ligand indicates a symmetrical distribution of the electron density with respect to the P-Mo-P plane. Fig. 3c is the typical MESP painted van der Waals surface of the complex wherein the violet region around the hydride ligand appears as the most electron rich. For all the metal hydride complexes, negative-valued V_{min} is always observed for the hydride ligand. In the following section, V_{min} features will be discussed for various systems.

MESP analysis of Mn Mo, W, Re, Fe and Ru hydride complexes

The MESP is very sensitive to electronic perturbations in a molecule and hence variations in the ligand environment can cause subtle changes in the MESP value around the hydride ligand. This can be easily proved by analyzing the V_{min} of all the metal hydride complexes (Table 2). For instance, in the case of Mn complexes, **1** with five CO groups shows the lowest V_{min} -2.7 kcal/mol while complex **6** having only PH₃ ligands shows the most negative V_{min} -34.1 kcal/mol. The drastic change in V_{min} can be associated to the σ donating power of PH₃ ligand compared to the electron withdrawing character of CO. The V_{min} of **1**, **2**, **3**, and **4** are -2.7, -12.6, -22.7 and -32.9 kcal/mol, respectively which indicates that for substituting every CO by a PH₃, V_{min} becomes deeper by ~10 kcal/mol. Similar conclusion is valid for isomers of **1**, **2**, **3**, and **4**. For instance, V_{min} of **2a** is -12.5 kcal/mol while that of **3b** is -22.7 kcal/mol. Other examples for comparison are (**3a**, **4a**) and (**4b**, **5b**). In the case of the three isomers of tris-phosphine systems **4a**, **4b**, and **4c**, significantly more negative V_{min} is observed for **4c** which suggests that equatorial/axial orientation of the ligands also play a role in controlling the hydridic character. As we move from **3c** to **7**, enhancement of the negative character of V_{min} is observed which can be attributed to the chelating effect of the bidentate phosphine ligand. The **9** and **8** complexes are very similar except for the axial ligand, the former having N₂ has V_{min} -30.7 kcal/mol while the later having CO has V_{min} -29.9 kcal/mol. These results suggest that CO and N₂ have similar electronic effect on the hydridic character.

The V_{min} values clearly suggest that negative MESP around the hydride ligand undergoes remarkable changes with respect to the nature of the metal and its ligand environment. For instance, Re complexes show more negative V_{min} than Mn complexes. In general, going down the group enhances the negative character of V_{min}. Among the seven Re complexes, **17** has the maximum negative V_{min}. The V_{min} of **17** is more negative than V_{min} of its isomer **15** by 5.1 kcal/mol suggesting that the influence PH₃

ligand trans to the hydride ligand is more electron donating than the trans orienting N_2. The **11** exhibits the lowest V_{min} (-9.2 kcal/mol) which can be attributed to the electron withdrawing effect of CO ligands. Group VII complexes show a wide range of
5 V_{min} values due to the inclusion of various electron withdrawing/donating ligands.
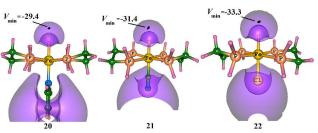
On the basis of V_{min}, the ligand environment of metal hydride complexes can be understood either as electron withdrawing or as electron donating. The V_{min} of a representative set of Mn and Fe
10 complexes are depicted in Fig. 4 along with a MESP isosurface of value -19.0 kcal/mol. The phosphine, CH, NO, bidentate chelating phosphine ligands and amino ligands show large negative values for V_{min} compared to other ligands. Such ligands could be treated as electron donating whereas the metal hydride
15 complexes containing CO, Cl, F and SiH_3 groups always show smaller negative V_{min} values. These ligands act as electron withdrawing and hence a decrease in the hydridic character is expected in the corresponding metal hydride complexes. In most cases, the donating cis ligands are more useful than trans
20 withdrawing ligands for improving hydridic character. For instance, **20**, **21** and **22** complexes have moderate V_{min} values with electron withdrawing group in the trans position.

In the case of tungsten complexes containing bulky triethyl-, trimethyl- and triphenyl phosphine ligands, the strong σ-donating
25 alkyl substitution on phosphorous is found to enhance V_{min} of the hydride ligand than the V_{min} of PH_3 ligand (s.i.). Such bulky ligands improve the hydridic character. Since MESP is a one electron property, it is well established that the absolute values as well as trends in V_{min} of molecules are largely unaffected by the
30 level of theory and basis set used.[65] In order to verify this, V_{min} of a representative set of Ru hydride complexes is evaluated using TPSS/aug-cc-pVDZ DFT method. At this level, the magnitude of V_{min} only slightly decreased and the overall trend of V_{min} remained unaffected compared to B3LYP results (s.i.).
35 The MESP at the hydride nucleus (V_H) is also very sensitive to the ligand environment as well as the metal center as it is varied from -685.2 to -759.1 kcal/mol (Table 2). The most negative and the least negative V_H are observed for **42** and **1**, respectively. In the case of Mn complexes, negative character of V_H is increased
40 with increase in the number of electron donating phosphine ligands (**1 – 6**). Very similar observation is also found in Re complexes (**11 – 17**).

V_{min} =-26.1 V_{min} =-27.4 V_{min} =-32.9

4a   4b   4c

V_{min} =-29.4 V_{min} =-31.4 V_{min} =-33.3

20   21   22

45 **Fig. 4** Isosurface plots of MESP (-19.0 kcal/mol) for isomeric hydride complexes of Mn and Fe. MESP minimum at the hydride ligand (V_{min}) in kcal/mol is also shown.
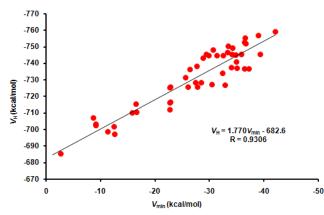

$V_H = 1.770 V_{min} - 682.6$
$R = 0.9306$

Fig. 5 The correlation between MESP at the hydride nucleus (V_H)
50 and MESP minimum at the hydride ligand (V_{min}) for all metal hydride complexes.

Electron donation of the phosphine in the equatorial position (cis to hydride ligand) is more effective than that in the axial
55 position (trans to hydride ligand). An electron withdrawing ligand trans to the hydride ligand increases the magnitude of V_H. For example, in Fe complexes **18** and **19** where trans ligand is Cl^- and F^-, respectively, V_H of **18** is -703.3 kcal/mol and that of **19** is -710.0 kcal/mol. This indicates that Cl^- has more electron
60 withdrawing power than F^-. Similar effect is observed for Ru complex **25** which has Cl^- in the equatorial position and shows V_H = -710.3 kcal/mol while the corresponding F^- derivative (**26**) shows V_H = -716.5 kcal/mol. The V_{min} and V_H values show a good linear correlation (Fig. 5). Previously we have shown that the
65 spatial quantity V_{min} is more sensitive to steric effect than the nuclear quantity V_H and hence the outliers seen in the linear trend can be attributed to the steric effect of the ligand environment on V_{min}.[35]

Stabilization energy of dihydrogen bonded hydride complexes
70 Recently, we have shown that the electron rich hydride ligand participates in dihydrogen H...H interactions with solvent water molecules and such interactions play significant role in water splitting reactions catalyzed by Ru pincer complex.[17] Following this work, the H...H interaction between a water molecule and the
75 hydride ligand in all the complexes is analyzed. An increase in the hydridic character is expected to increase the H...H interaction energy. Typical H...H distance (d_{HH}) in dihydrogen bonded complexes is in the range 1.6 to 2.2 Å[66-68] and all the d_{HH} values are found in the range 1.621 to 2.140 Å (Table 2). In general, the
80 d_{HH} decreases with increase in the negative character of V_{min} or V_H meaning that metal complexes showing strong hydridicity

enhance outersphere binding of water to the hydride complex (s.i.). Equatorial groups such as Cl, SiH$_3$, CNO, heterocyclic, and CO (in cis- or trans- position), increase d$_{HH}$. Ligands trans with respect to hydride, *viz.* NO and CH as well as bidentate P and N ligands decrease d$_{HH}$. The orientation of water in the dihydrogen complex can be measured in terms of the M-H…H angle θ and H…H-O angle Ψ. The θ values are in the range 120-145º while ψ values vary from 109 to 178º (Table 2). The Ψ is found to be more linear with more negative V_H (correlation coefficient = 0.920).
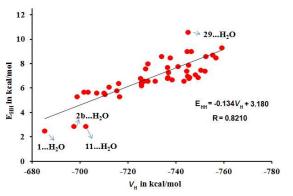
Experimental studies reveal that the stabilizing energies of H…H bonded complexes (E$_{HH}$) is in the range 2 - 7 kcal/mol.[66, 67] In this study, E$_{HH}$ is found in the range 2.5 to 13.2 kcal/mol and several complexes have E$_{HH}$ values higher than the typically observed experimental values. 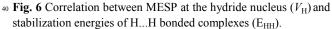The highest E$_{HH}$ value is observed for **29…H$_2$O** (10.6 kcal/mol). In general, E$_{HH}$ increases with increase in the negative character of V_H (Fig. 6) which means that more hydridic character of the ligand promotes H…H dihydrogen interaction. This result is important because it suggests that the electron rich character of the hydride ligand assessed in terms of V_H is useful to make a good prediction on the power of the hydride ligand to interact with a water molecule through dihydrogen bond. The prediction is only qualitative because E$_{HH}$ does not fully account for the dihydrogen bond energy. In many cases, apart from dihydrogen interactions, secondary interactions involving oxygen of water contributes to E$_{HH}$. Representative two Ru hydride complexes showing this feature is given in Fig. 7. Secondary interactions arise between oxygen of water and hydride of the equatorial chelating ligands or between the hydride of water and oxygen of the equatorial CO ligands. Other examples showing secondary interactions are **7…H$_2$O, 8…H$_2$O, 9…H$_2$O, 21…H$_2$O, 33…H$_2$O, 35…H$_2$O, 41…H$_2$O** and **42…H$_2$O**. In **1…H$_2$O, 11…H$_2$O** and **2b…H$_2$O** dihydrogen bond formation is not observed as the water molecule preferred an interaction with the carbonyl than the hydride.

Table 2. Structural parameters and binding energies (kcal/mol) of all dihydrogen bonded complexes. Dihydrogen distance, d$_{H-H}$ in Å and angles (Ψ$_{(H…H-O)}$ and θ$_{(M-H…H)}$) in degree. The V_{min} and V_H of the parent complexes (kcal/mol) are also given.

Models	d$_{H-H}$	Ψ	Θ	E$_{HH}$	V_{min}	V_H	Models	d$_{H-H}$	Ψ	θ	E$_{HH}$	V_{min}	V_H
1…H$_2$O	2.861	109.0	120.7	2.5	-2.7	-685.2	19…H$_2$O	1.817	156.4	120.4	5.6	-15.8	-710.0
2a…H$_2$O	2.039	141.3	126.7	5.7	-12.5	-701.6	20…H$_2$O	1.651	177.3	126.7	6.9	-29.4	-745.5
2b…H$_2$O	2.143	142.3	127.2	2.9	-12.6	-697.3	21…H$_2$O	1.636	177.4	120.5	9.0	-31.4	-744.7
3a…H$_2$O	1.933	153.2	123.4	5.8	-16.5	-715.3	22…H$_2$O	1.635	178.8	121.7	9.0	-33.3	-746.4
3b…H$_2$O	1.896	148.8	128.5	6.1	-22.7	-712.1	23…H$_2$O	2.062	146.0	118.2	5.6	-8.7	-707.0
3c…H$_2$O	1.669	161.7	124.8	6.4	-22.7	-716.1	24…H$_2$O	2.052	149.0	117.0	5.3	-11.3	-698.8
4a…H$_2$O	1.860	157.5	124.5	6.4	-26.1	-725.5	25…H$_2$O	2.006	152.6	117.7	5.5	-16.6	-710.3
4b…H$_2$O	1.648	168.0	124.4	6.6	-27.4	-728.2	26…H$_2$O	1.811	153.3	125.2	5.3	-22.8	-716.5
4c…H$_2$O	1.632	166.4	127.9	6.6	-32.9	-726.8	27…H$_2$O	1.727	173.4	116.7	6.5	-27.8	-725.8
5a…H$_2$O	1.642	172.8	120.6	6.7	-27.7	-738.3	28…H$_2$O	1.718	172.7	113.0	8.5	-34.0	-737.5
5b…H$_2$O	1.630	172.5	127.1	6.9	-37.2	-736.6	29…H$_2$O	1.720	169.7	110.4	10.6	-34.8	-745.1
6…H$_2$O	1.641	177.6	122.3	6.9	-34.1	-745.5	30…H$_2$O	1.720	175.1	118.6	7.7	-36.5	-736.5
7…H$_2$O	1.669	170.8	128.9	8.0	-28.5	-728.3	31…H$_2$O	1.793	162.8	116.0	6.6	-25.6	-731.3
8…H$_2$O	1.630	176.5	138.4	7.4	-29.9	-744.5	32…H$_2$O	1.661	169.5	132.2	8.6	-32.4	-734.0
9…H$_2$O	1.621	173.9	144.9	7.1	-30.7	-748.1	33…H$_2$O	1.669	168.2	115.5	7.8	-35.0	-740.8
10…H$_2$O	1.634	174.6	122.6	6.6	-28.9	-743.2	34…H$_2$O	1.627	177.2	128.5	8.6	-36.4	-752.5
11…H$_2$O	2.163	143.1	115.3	2.9	-9.2	-702.4	35…H$_2$O	1.665	171.8	114.2	7.4	-36.7	-752.0
12…H$_2$O	1.751	164.2	126.4	6.2	-22.9	-725.6	36…H$_2$O	1.623	177.5	128.3	8.5	-39.0	-756.7
13…H$_2$O	1.701	163.3	117.9	7.6	-30.4	-727.2	37…H$_2$O	1.863	154.0	117.3	6.8	-22.7	-725.2
14…H$_2$O	1.685	176.2	115.8	7.0	-32.5	-744.8	38…H$_2$O	1.815	161.2	115.7	6.8	-26.4	-736.4
15…H$_2$O	1.684	178.3	117.4	6.9	-34.2	-749.2	39…H$_2$O	1.681	171.2	114.9	7.5	-33.5	-750.4
16…H$_2$O	1.689	169.9	116.8	7.3	-35.1	-736.9	40…H$_2$O	1.682	166.5	116.1	7.9	-35.9	-745.2
17…H$_2$O	1.685	178.4	118.7	6.8	-39.3	-745.4	41…H$_2$O	1.640	179.0	124.7	8.7	-36.6	-755.2
18…H$_2$O	1.971	150.9	118.1	5.7	-9.2	-703.3	42…H$_2$O	1.630	179.2	123.2	9.3	-42.1	-759.1

Fig. 6 Correlation between MESP at the hydride nucleus (V_H) and stabilization energies of H…H bonded complexes (E$_{HH}$).

Designing metal hydride complexes for water splitting reactions

Experimentally it is known that tris- and bis-(trimethyl phosphine) W hydride complexes and bidentate Mo, W and Fe hydride complexes are useful for liberating hydrogen from water.[18, 23] It is also established that increasing hydridic character favours protonation from organic molecules leading to dihydrogen complex formation.[26] Strong hydridic character of a metal hydride can promote hydrogen release through a water

splitting outer sphere mechanism.[17] From the knowledge of V_{min} or V_H (Table 2) we may assess that **5b** and **6** from group VII and **22** from group 8 and **35**, **36**, **41** and **42** from group VI have high hydridic character and hence they may show higher tendency for water splitting reactions.

The applicability of V_{min} or V_H for tuning the activation barrier of H$_2$ elimination is tested by transition state modeling for group VI complexes. Large negative MESP values and weak M-H bond

strength are main reason for selecting group VI complexes. A representative example of **42** giving the details of the outer sphere mechanism is presented in Fig. 8. The dihydrogen complex passes through a 4-center transition state to yield the hydroxide
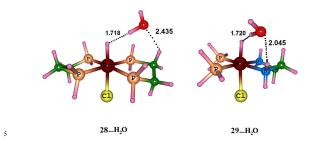

Fig. 7 Water adducts of Ru hydride complexes. Distance in Å.

metal complex. This type of a mechanism was previously discussed for bis-, tris-, and tetrakis- phosphine complexes of W, Mo and Cr.[19]
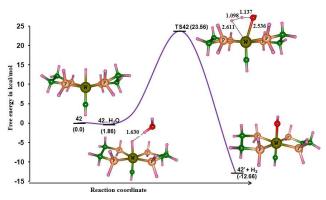

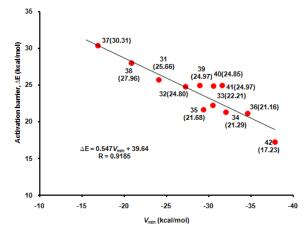**Fig. 8** Relative free energy profile of a representative system for hydrogen elimination.

Fig. 9 Correlation between activation barrier (ΔE) and MESP minimum at the hydride ligand (V_{min}) of W hydride complexes.

Fig. 9 depicts a correlation between activation energy (ΔE) for H_2 elimination and hydridic descriptor V_{min} of group VI complexes. The correlation coefficient 0.9185 suggests a decreasing linear trend in activation barrier with increase in the negative V_{min} meaning that water splitting becomes easy with more electron rich hydride ligand. Complex **42** showed the lowest energy

barrier of 17.23 kcal/mol compared to any other systems. In this complex, trans CH and chelating ligands enhance electron density at hydride leading to decrease in the activation barrier. Complex **37** contains three CO ligands and shows a high energy barrier 30.31 kcal/mol. Chelating phosphine ligands in **32**, **34**, **36**, **41** and **42** enhance negative V_{min} and they show activation barrier below 25 kcal/mol. In **31** and **38**, CO ligand decreases hydridicity and the corresponding activation barriers are also high, *viz.* 27.96 and 25.66 kcal/mol, respectively. In general, ligands such as CH, NO orienting trans to the hydride ligand and phosphines, cis-chelating bidentate phosphine and amine groups are good for lowering the activation barrier.

Conclusions

In summary, the structural and electronic features of a large variety of metal hydride complexes wherein the metal is Mo, W, Mn, Re, Fe and Ru have been studied using DFT. In all complexes, MESP topography revealed that the hydride ligand possesses a characteristic negative minimum V_{min}. The value of V_{min} is useful to estimate the hydridic character (electron rich character) of that ligand. The hydridic nature of the ligand is also measured in terms of MESP at the hydride nucleus (V_H). The V_{min} and V_H are very sensitive to the ligand environment. Hence, by monitoring the MESP that surrounds the hydride ligand, fine tuning of the ligand environment is possible. As V_{min} of the hydride ligand becomes more negative, its interaction with a water molecule for dihydrogen bonding becomes higher leading to facile release of H_2 from the complex. A more electron rich hydride ligand showed lower activation barrier for H_2 elimination. Thus V_{min} and V_H are proposed as two useful electronic descriptors for the study of the hydridic character of a metal hydride complex. Since MESP analysis provides more insight into the interactive behaviour of the metal hydride complex with a water molecule, tuning the ligand environment for more negative V_{min} or V_H is attractive to design new water splitting metal hydride complexes.

Reference

1. M. Ito, M. Hirakawa, K. Murata and T. Ikariya, *Organometallics*, 2001, **20**, 379-381.
2. B. Liu, Y. Gao, X. Zhao, W. Yan and X. Wang, *J. Polym. Sci., Part A: Polym. Chem.*, 2010, **48**, 359-365.
3. R. Noyori, M. Yamakawa and S. Hashiguchi, *J. Org. Chem.*, 2001, **66**, 7931-7944.
4. J. C. Taylor and G. D. Markham, *J. Biol. Chem.*, 1999, **274**, 32909-32914.
5. P. Woolley, *J. Chem. Soc., Chem. Commun.*, 1975, 579-580.
6. P. Margl, T. Ziegler and P. E. Blöchl, *J. Am. Chem. Soc.*, 1996, **118**, 5412-5419.
7. M. L. Helm, M. P. Stewart, R. M. Bullock, M. R. DuBois and D. L. DuBois, *Science*, 2011, **333**, 863-866.

Dalton Transactions

Page 8 of 10

8. U. J. Kilgore, M. P. Stewart, M. L. Helm, W. G. Dougherty, W. S. Kassel, M. R. Dubois, D. L. Dubois and R. M. Bullock, *Inorg. Chem.*, 2011, **50**, 10908-10918.

9. A. Boddien, D. Mellmann, F. Gartner, R. Jackstell, H. Junge, P. J. Dyson, G. Laurenczy, R. Ludwig and M. Beller, *Science*, 2011, **333**, 1733-1736.

10. I. Mellone, M. Peruzzini, L. Rosi, D. Mellmann, H. Junge, M. Beller and L. Gonsalvi, *Dalton Trans.*, 2013, **42**, 2495-2501.

11. S. Musa, I. Shaposhnikov, S. Cohen and D. Gelman, *Angew. Chem. Int. Ed.*, 2011, **50**, 3533-3537.

12. M. Nielsen, A. Kammer, D. Cozzula, H. Junge, S. Gladiali and M. Beller, *Angew. Chem. Int. Ed.*, 2011, **50**, 9593-9597.

13. S. C. Marinescu, J. R. Winkler and H. B. Gray, *Proc. Natl. Acad. Sci. U.S.A.*, 2012, **109**, 15127-15131.

14. S. W. Kohl, L. Weiner, L. Schwartsburd, L. Konstantinovski, L. J. W. Shimon, Y. B. David, M. A. Iron and D. Milstein, *Science*, 2009, **324**, 74-77.

15. X. Yang and M. B. Hall, *J. Am. Chem. Soc.*, 2010, **132**, 120–130.

16. J. Li, Y. Shiota and K. Yoshizawa, *J.Am.Chem.Soc.*, 2009, **131**, 13584-13585.

17. K. S. Sandhya and C. H. Suresh, *Organometallics*, 2011, **30**, 3888-3891.

18. N. Avramović, J. Höck, O. Blacque, T. Fox, H. W. Schmalle and H. Berke, *J. Organomet. Chem.*, 2010, **695**, 382-391.

19. K. S. Sandhya and C. H. Suresh, *Dalton Trans.*, 2012, **41**, 11018-11025.

20. V. A. Levina, A. Rossin, N. V. Belkova, M. R. Chierotti, L. M. Epstein, O. A. Filippov, R. Gobetto, L. Gonsalvi, A. Lledõs, E. S. Shubina, F. Zanobini and M. Peruzzini, *Angew. Chem. Int. Ed.*, 2011, **50**, 1367-1370.

21. N. V. Belkova, A. V. Ionidis, L. M. Epstein, E. S. Shubina, S. Gruendemann, N. S. Golubev and H. H. Limbach, *Eur. J. Inorg. Chem.*, 2001, 1753-1761.

22. N. V. Belkova, P. O. Revin, M. Besora, M. Baya, L. M. Epstein, A. Lledós, R. Poli, E. S. Shubina and E. V. Vorontsov, *Eur. J. Inorg. Chem.*, 2006, 2192-2209.

23. N. V. Belkova, P. O. Revin, L. M. Epstein, E. V. Vorontsov, V. I. Bakhmutov, E. S. Shubina, E. Collange and R. Poli, *J. Am. Chem. Soc.*, 2003, **125**, 11106-11115.

24. N. V. Belkova, P. A. Dub, M. Baya and J. Houghton, *Inorg. Chim. Acta.*, 2007, **360**, 149-162.

25. N. K. Szymczak and D. R. Tyler, *Coord. Chem. Rev.*, 2008, **252**, 212-230.

26. R. Custelcean and J. E. Jackson, *Chem. Rev.*, 2001, **101**, 1963-1980.

27. W. Z. Li, T. Liu, J. B. Cheng, Q. Z. Li and B. A. Gong, *J. Organomet. Chem.*, 2010, **695**, 909-912.

28. P. Politzer and D. G. Truhlar, eds., *Chemical Applications of Atomic and Molecular Electrostatic Potentials*, Plenum Press, New York, 1981.

29. S. R. Gadre and R. N. Shirsat, *Electrostatics of Atoms and Molecules*, Universities Press, Hyderabad, India 2000

30. P. Sjoberg and P. Politzer, *J. Phys. Chem.*, 1990, **94**, 3959-3961.

31. S. Maheshwary, N. Patel, N. Sathyamurthy, A. D. Kulkarni and S. R. Gadre, *Journal of Physical Chemistry A*, 2001, **105**, 10525-10537.

32. S. R. Gadre and P. K. Bhadane, *J. Phys. Chem. A*, 1999, **103**, 3512-3517.

33. S. S. Pundlik and S. R. Gadre, *J. Phys. Chem. B*, 1997, **101**, 9657-9662.

34. V. Dimitrova, S. Ilieva and B. Galabov, *J. Phys. Chem. A*, 2002, **106**, 11801-11805.

35. J. Mathew and C. H. Suresh, *Organometallics*, 2011, **30**, 1438-1444.

36. C. H. Suresh, N. Koga and S. R. Gadre, *J. Org. Chem.*, 2001, **66**, 6883-6890.

37. F. B. Sayyed and C. H. Suresh, *Tetrahedron Lett.*, 2009, **50**, 7351-7354.

38. S. R. Gadre and P. K. Bhadane, *J. Chem. Phys.*, 1997, **107**, 5625-5626.

39. B. Galabov, S. Ilieva, G. Koleva, W. Allen, H. F. Schaefer III and P. v. R. Schleyer, *WIRES Comput. Mol. Sci.*, 2013, **3**.

40. B. Galabov, V. Nikolova and S. Ilieva, *Chem. Eur. J.*, 2013, **19**, 5149-5155.

41. S. Ilieva, D. Nalbantova, B. Hadjieva and B. Galabov, *J. Org. Chem.*, 2013, **78**, 6440-6449.

42. D. J. Darensbourg, P. Ganguly and D. R. Billodeaux, *Organometallics*, 2004, **23**, 6025-6030.

43. D. Nietlispach, D. Veghini and H. Berke, *Helv Chimi Acta*, 2004, **77**, 2197-2208.

44. F. P. Liang, H. Jacobsen, H. W. Schmalle, T. Fox and H. Berke, *Organometallics*, 2000, **19**, 1950-1962.

45. G. Wagner and W. Hieber, *Z. Naturforsch. B*, 1958, **13**, 338.

46. M. J. Frisch, G. W. Trucks, H. B. Schlegel, G. E. Scuseria, M. A. Robb, J. R. Cheeseman, G. Scalmani, V. Barone, B. Mennucci, G. A. Petersson, H. Nakatsuji, M. Caricato, X. Li, H. P. Hratchian, A. F. Izmaylov, J. Bloino, G. Zheng, J. L. Sonnenberg, M. Hada, M. Ehara, K. Toyota, R. Fukuda, J. Hasegawa, M. Ishida, T. Nakajima, Y. Honda, O. Kitao, H. Nakai, T. Vreven, J. Montgomery, J. A. , J. E. Peralta, F. Ogliaro, M. Bearpark, J. J. Heyd, E. Brothers, K. N. Kudin, V. N. Staroverov, T. Keith, R. Kobayashi, J. Normand, K. Raghavachari, A. Rendell, J. C. Burant, S. S. Iyengar, J. Tomasi, M. Cossi, N. Rega, J. M. Millam, M. Klene, J. E. Knox, J. B. Cross, V. Bakken, C. Adamo, J. Jaramillo, R. Gomperts, R. E. Stratmann, O. Yazyev, A. J. Austin, R. Cammi, C. Pomelli, J. W. Ochterski, R. L. Martin, K. Morokuma, V. G. Zakrzewski, G. A. Voth, P. Salvador, J. J. Dannenberg, S. Dapprich, A. D. Daniels, O. Farkas, J. B. Foresman, J. V. Ortiz, J. Cioslowski and D. J. Fox, Gaussian, Inc. , Gaussian 09, Wallingford CT Revision C.01 edn., 2010.

47. A. D. Becke, *J. Chem. Phys.*, 1993, **98**, 5648.

48. C. Lee, W. Yang and R. G. Parr, *Phys. Rev. B*, 1988, **37**, 785-789.

49. P. J. Hay and W. R. Wadt, *J. Chem. Phys.*, 1985, **82**, 299-310.

50. A. W. Ehlers, M. Biihme, S. Dapprich, A. Gobbi, A. Hijllwarth, V. Jonas, K. F. Kiihler, R. Stegmann, A. Veldkamp and G. Frenking, *Chem. Phy. Lett.*, 1993, **208**, 111-114.

51. P. C. Hariharan and J. A. Pople, *Theor. Chim. Acta*, 1973, **28**, 213-222.

52. P. J. Hay and W. R. Wadt, *Chin. J. Chem. Phys.*, 1985, **82**, 270-283.

53. H. P. Hratchian and H. B. Schlegel, *J. Chem. Phys.*, 2004, **120**, 9918-9942.

54. S. F. Boys and F. Bernardi, *Mol.Phys.*, 1970, **19**, 553-566.

55. C. H. Suresh, *Inorg. Chem.*, 2006, **45**, 4982-4986.

56. N. Fey, *Dalton Trans.*, 2010, **39**, 296-310.

57. N. Fey, A. G. Orpen and J. N. Harvey, *Coord. Chem. Rev.* , 2009, **253**, 704-722.

5 58. J. Jover, N. Fey, J. N. Harvey, G. C. Lloyd-Jones, A. G. Orpen, G. J. J. Owen-Smith, P. Murray, D. R. J. Hose, R. Osborne and M. Purdie, *Organometallics*, 2010, **29**, 6245-6258.

59. Y. A. Abramov, L. Brammer, W. T. Klooster and R. Morris Bullock, *Inorg. Chem.*, 1998, **37**, 6317-6328.

10 60. E. S. Shubina, N. V. Belkova, A. N. Krylov, E. V. Vorontsov, L. M. Epstein, D. G. Gusev, M. Niedermann and H. Berke, *J. Am. Chem. Soc.*, **1996**, *118*, 1105-1112.

61. A. A. H. Van der Zeijden, B. H. Wllllam and H. Berke, *Organometallics*, 1992, **11**, 563-513

15 62. G. L. Hillhouse and B. Haymore, L, *Inorg. Chem.*, 1987, **26**, 1876-1885.

63. P. K. Sajith and C. H. Suresh, *Dalton Trans.*, 2010, **39**, 815-822.

64. N. Mohan, C. H. Suresh, A. Kumar and S. R. Gadre, *Phys. Chem. Chem. Phys.*, 2013, **15**, 18401-18409.

20 65. S. R. Gadre, S. A. Kulkarni, C. H. Suresh and I. H. Shrivastava, *Chem. Phys. Lett.*, 1995, **239**, 273-281.

66. E. Peris, J. C. Lee Jr, J. R. Rambo, O. Eisenstein and R. H. Crabtree, *J. Am. Chem. Soc.*, 1995, **117**, 3485-3491.

67. P. Desmurs, K. Kavallieratos, W. Yao and R. H. Crabtree, *New J. Chem.*, 1999, **23**, 1111-1115.

68. T. B. Richardson, T. F. Koetzle and R. H. Crabtree, *Inorg. Chim. Acta*, 1996, **250**, 69-73.

Designing metal hydride complexes for water splitting reactions: A molecular electrostatic potential approach

K. S. Sandhya,[a] **and Cherumuttathu H. Suresh***[a]

Graphical Abstract

Molecular electrostatic potential minimum of   metal-hydrides (V_{min}) is used as a sensitive electronic descriptor to tune H_2 elimination reactions.